Supplementary Information

Heparin Binding Induced Supramolecular Chirality into Self-Assembly of Perylenediimide bolaamphiphile

Poonam Sharma,[a,†] Akhil Venugopal,[a,b,†] Claudia Martínez Verdi,[a] Mauri Serra Roger,[a] Annalisa Calò[b,c,d] and Mohit Kumar*[a,b,e]

[a]*Department of Inorganic and Organic Chemistry, University of Barcelona, Calle Marti i Fraquès 1-11, 08028 Barcelona (Spain). Email: mohit.kumar@ub.edu*

[b]*Institute for Bioengineering of Catalonia (IBEC), Calle Baldiri Reixac 10–12, 08028 Barcelona (Spain)*

[c]*Department of Electronic and Biomedical Engineering, University of Barcelona, Calle Marti i Fraquès 1-11, 08028 Barcelona (Spain)*

[d]*Institute of Nanoscience and Nanotechnology, University of Barcelona, 08028 Barcelona (Spain)*

[e]*Institut de Química Teòrica i Computacional, University of Barcelona, 08028 Barcelona (Spain)*

Table of Contents

1. Materials and methods

All the solvents and reagents were commercially available and used as received unless otherwise specified. DMSO was obtained from Carlo Erba reagents. 3,4,9,10-Perylenetetracarboxylic dianhydride was obtained from sigma-aldrich and heparin sodium salt derived from porcine intestinal mucosa was purchased from thermo fisher scientific. FBS medium was obtained from thermo fisher scientific.

Stock Solution preparation

For all measurements, stock solution of derivative **1** was prepared in DMSO (5 mM). The final concentration of all samples for study was 0.05 mM in different DMSO-water ratios. The heparin stock solution of 25.8 mg/ml was prepared by dissolving 5.16 mg in 200 µL of milli-Q water. Foetal Bovine Serum (FBS) was prepared under sterile conditions. The commercial FBS was diluted ten times in milli-Q water which was used for the measurements.

NMR

The ^{1}H NMR spectral measurement were recorded on VARIAN MERCURY 400 spectrometer using DMSO-d_6 and D_2O as a solvent. Chemical shift (δ) values are reported in ppm.

UV-Visible absorption spectroscopy

2.5 ml samples were placed in glass cuvette of 1 cm path length to measure the UV-Visible absorbance spectra with an Agilent Cary 5000 spectrophotometer at a scanning speed of 600 nm per minute. We used glass cuvettes, knowing the fact that glass only absorbs in the UV region below 320 nm. However, we recorded the spectra in the range of 400-750 nm.

Fluorescence spectroscopy

250 µl samples were placed in 1 mm quartz cuvette to measure the fluorescence spectra in front face excitation geometry using Photon Technology International (PTI) fluorometer which uses a xenon arc lamp light source. The excitation wavelength was 465 nm. We used front face geometry to record the data to avoid inner filter effects.

Quantum yield measurements

Fluorescence quantum yields (ΦS) were determined by using an optically matching solution of Rhodamine B (ΦR = 0.49 in ethanol) as standard at excitation wavelength of 500 nm and quantum yield is calculated using equation:

$$\Phi_S = \Phi_R \times \eta S^2/\eta R^2 \times D_S A_R/D_R A_S$$

Φ_S and Φ_R are the quantum yields of sample and reference, respectively. D_S and D_R are the respective areas of emission for the sample and reference, respectively. A_S and A_R are the absorbance; ηS and ηR are the refractive indices[1] of the sample and reference solutions, respectively

Circular Dichroism

The circular dichroism spectra were recorded using a Jasco J-815 spectropolarimeter (Serial no. A009761168) with a wavelength range of 190-800 nm. Sample solutions were prepared at a concentration of 0.05 mM in different water ratios in DMSO and placed in a glass cuvette with a path length of 1 cm. Spectra were recorded at a scan speed of 200 nm/min. Data analysis included baseline correction by subtracting the blank solution. The data was smoothened using 5 points of Savitzky-Golay method.

Size and Zeta-Potential (ζ-Potential)

Zetasizer Nano-ZS Malvern Instrument equipped with a built-in temperature controller was employed for dynamic light scattering (DLS) particle size experiment. For size distribution, an average of 10 measurements were considered as the data. Size distribution data was collected for molecule **1** with or without addition of heparin at 25.0 ± 0.1°C. And the ζ-potential measurements were carried out using a Microtrac Stabino Zeta Analyzer. All measurements were performed at a fixed temperature of 20.0 ± 0.1 °C. The samples were prepared at 0.05 mM concentration in 50% and 99% water, providing insights into surface charge properties.

Atomic Force Microscopy (AFM)

AFM images were recorded using a Nanowizard 4 Bio-AFM (JPK-Bruker) working in tapping mode, using cantilever Tap150 Al-G (BudgetSensors) (f = 140 kHz, A_{free} = 25 nm, $A_{setpoint}$ = 10 nm). Measurements were performed in the air. Samples for AFM analysis were prepared in Milli-Q water. 50 µL of solution was drop casted on freshly cleaved mica, allowed to dry in air for 2 hrs, and then kept in desiccator for complete drying before imaging.

Transmission Electron microscopy (TEM)

The TEM images were recorded on a Jeol J1010 microscope operating at an accelerating voltage of 80 kV. The samples for TEM analysis were prepared by drop casting 10 µL aliquot of the sample solution

on a carbon film grid (400 mesh, copper) and dried for two minutes. Then excess sample solution was wicked off with filter paper and dried completely. Then, 10 µL uranyl acetate stain (2% solution) was drop casted, blotted away after 30 seconds, and dried completely. The grid was then air dried at room temperature overnight before imaging.

2. Synthesis

Amphiphilic dicationic perylene diimide (PDI) derivative **1** was synthesized according to the literature methods.[1]

3. Supplementary Figures

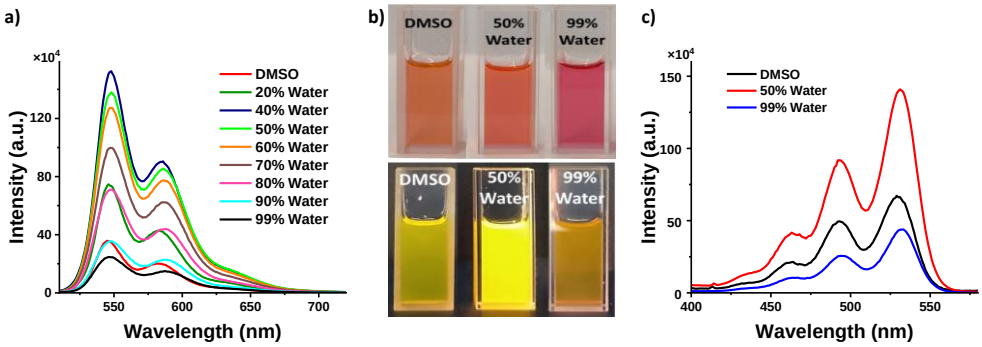

Figure S1. (a) Fluorescence spectra of derivative **1** (0.05 mM) in varying % of water in DMSO; (b) Photographs showing colour change of derivative **1** (0.05 mM) under ambient conditions and under 365 nm light in DMSO, 50% of H_2O and 99% of H_2O in DMSO; (c) Excitation spectra of derivative **1** (0.05 mM) collected at 600 nm in DMSO, 50% and 99% of H_2O in DMSO showing that the emission comes only from the residual monomers in solution (λ_{ex}= 600 nm).

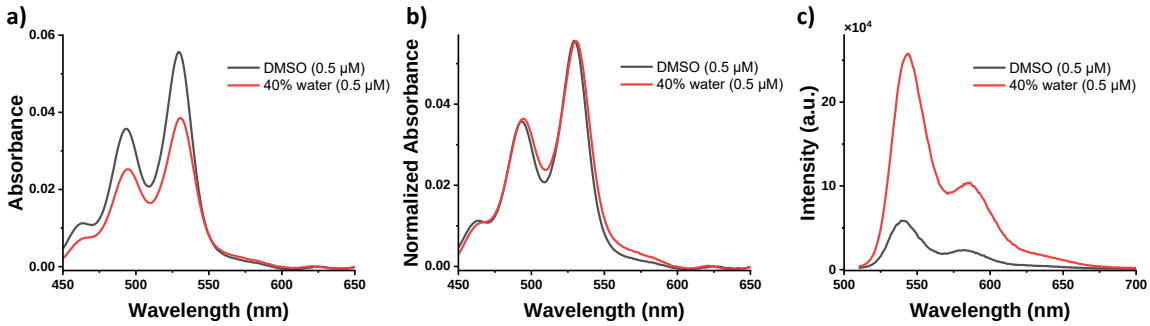

S. No.	Solvent System	Concentration of molecule 1	Quantum Yield (%)
1.	DMSO	0.5 µM	7
2.	40% water-DMSO mixture	0.5 µM	44

Figure S2. (a) Absorption spectra; (b) normalized absorption spectra and (c) emission spectra of **1** at very low concentration (0.5 µM) in DMSO and 40% water in DMSO solvent compositions. From (a) and (b) it is evident that molecule **1** is completely monomeric in very low concentration of 0.5 µM in both the solvent compositions i.e. in DMSO and 40% water in DMSO. Therefore, the concentration of monomer is same in the two solvents. However, the emission spectra in (c) shows that the emission intensity is 4.4 times higher in 40% water in DMSO when compared to DMSO. Below is the table showing the quantum yield calculations in two solvent compositions confirming that the inherent quantum yield of monomers of **1** is higher in 40% water in DMSO when compared to DMSO.

To understand the unexpected observation of high fluorescence of **1** in 40% water compared to DMSO alone even though there are lower concentration of monomers in 40% water, we performed spectroscopic studies in these two solvents at very low concentrations. We diluted the sample 100 times to 0.5 μM such that **1** is completely monomeric in DMSO as well as in 40% DMSO, as confirmed by the absorption and emission spectra (Figure S2). Here since the concentration of monomer is the same in both solvents, we observed that the monomeric emission intensity is 4.4 times higher in 40% water compared to pure DMSO. Additionally, we measured the quantum yield of the monomers in these two solvent compositions, using Rhodamine B as the standard, and found that the quantum yield in DMSO is 7% whereas in 40% water it is more than 6 times higher i.e. 44%. Thus, the inherent quantum yield of monomer **1** is high in 40% water than in water. It is known in literature that the quantum yield of a compound can be dependent on the solvent medium.

Therefore, at our working concentration in the manuscript (0.05 mM) even though there are more monomers in DMSO compared to 40% water sample, the emission intensity in 40% water is higher due to the inherently high quantum yield of the monomers in 40% water compared to DMSO alone.

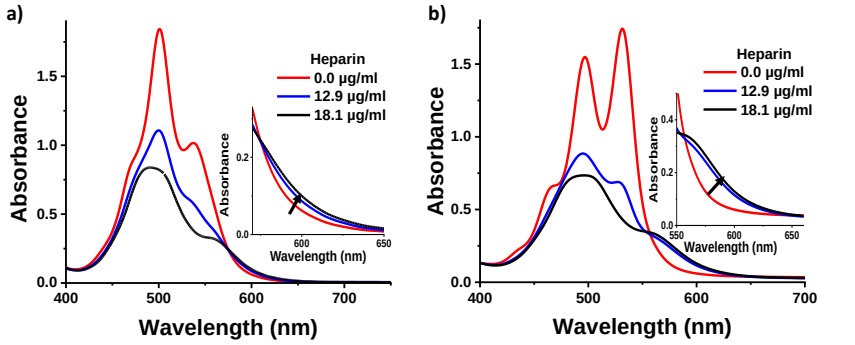

c) 99% aqueous medium	
Heparin (mg/ml)	$S_{0\text{-}0}/S_{0\text{-}1}$
0	0.7
12.9	0.5
18.1	0.5

d) 50% aqueous medium	
Heparin (mg/ml)	$S_{0\text{-}0}/S_{0\text{-}1}$
0	1.3
12.9	0.8
18.1	0.6

Figure S3. Absorption spectral changes of derivative **1** (0.05 mM) before and after the addition of heparin in (a) 99% water and (b) 50% water. [inset of (a) and (b) showing absorption changes at 600 nm due to heparin binding]; and Summary table showing variation of ratios of $S_{0\text{-}0}/S_{0\text{-}1}$ absorption bands of derivative **1** before and after the addition of heparin in (c) 99% water and (d) 50% water.

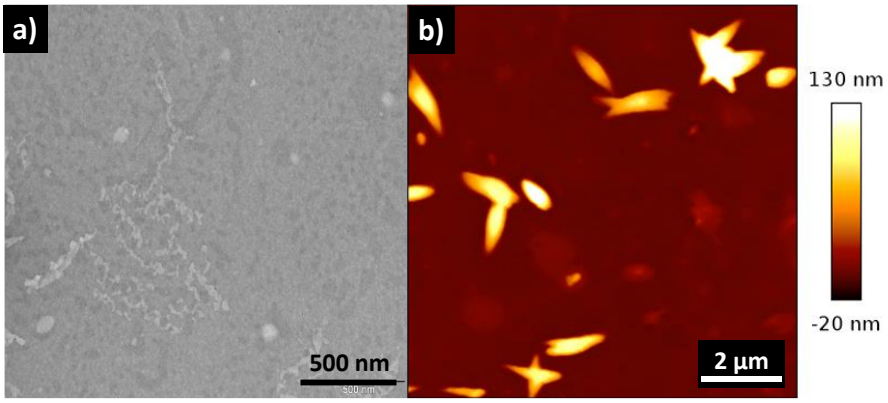

Figure S4. (a) Transmission Electron Microscopy (TEM) and (b) Atomic force microscopy (AFM) images of derivative **1** (0.05 mM) in 99% water.

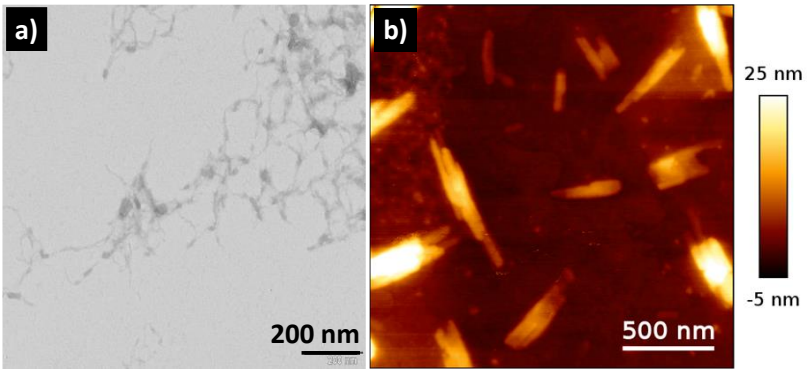

Figure S5. (a) Transmission Electron Microscopy (TEM) and (b) Atomic force microscopy (AFM) images of **1** (0.05 mM) in the presence of heparin showing heparin-induced self-assembly of **1**. Concentration of **1** = 0.05 mM; solvent: 99% water in DMSO, concentration of heparin= 25.8 µg/ml and the staining agent = 2% uranyl acetate.

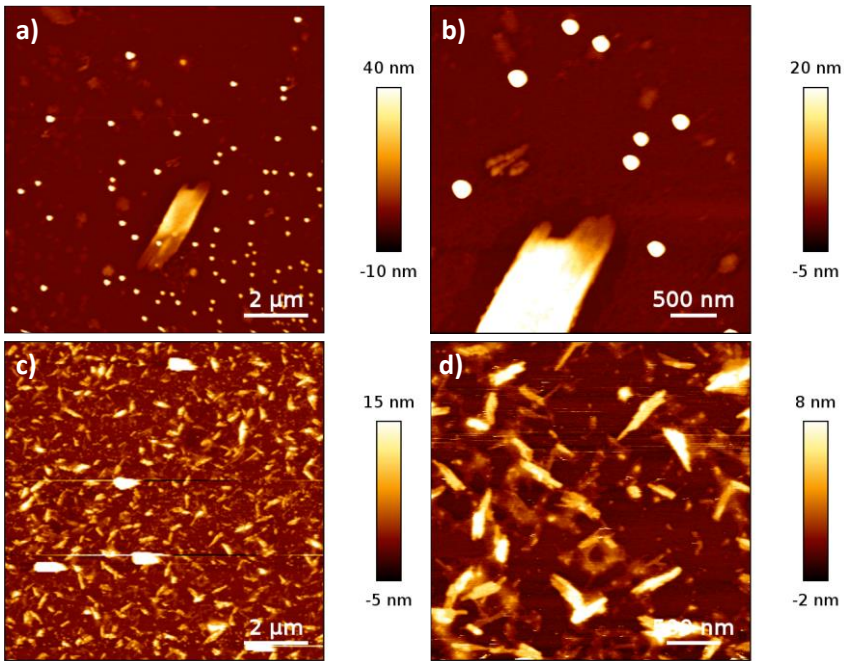

Figure S6. AFM images of **1** from other area of mica sheet before (a,b) and after (c,d) the addition of heparin. Concentration of **1** = 0.05 mM; solvent: 99% water in DMSO, concentration of heparin= 25.8 µg/ml.

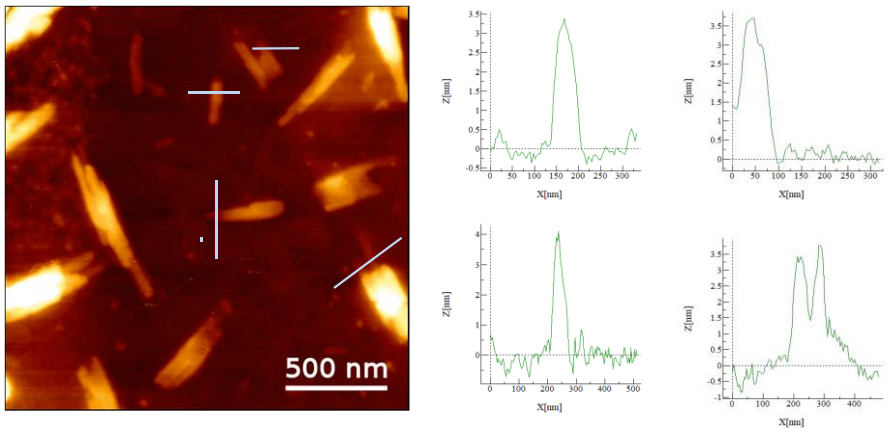

Figure S7. (a) Height profile analysis of AFM images of heparin induced self-assembled supramolecular polymeric structures showing molecular organization within the nanostructures.

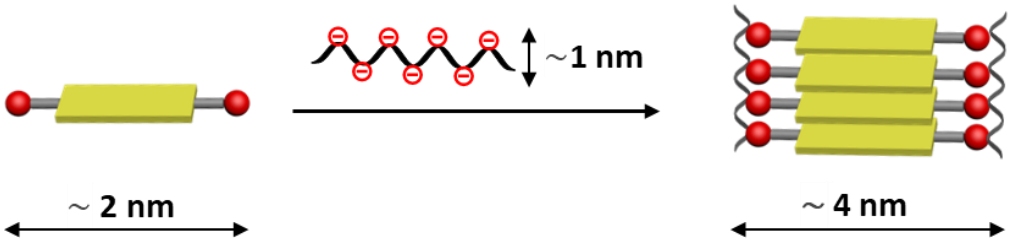

Scheme S1. (a) Schematic view of molecular organization and dimensions of fibres of **1** and heparin induced self-assembled supramolecular polymeric structures.

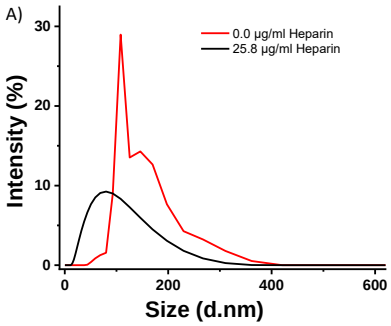

Figure S8. DLS analysis showing variation of size of self-assembled **1** in the presence of 2 equivalents of heparin. Concentration of **1** = 0.05 mM; solvent: 99% water in DMSO.

Dynamic light scattering (DLS) experiments were also performed to check the change in size upon addition of heparin. We observe a broad bimodal size distribution of self-assembled **1** which changes to monomodal size upon binding with heparin. This indicates supramolecular transformation. We would like to point out that DLS is not an ideal technique for characterizing fibrous (fibrillar) nanostructures as they do not fit very well into the spherical model used in DLS. Even with these limitations we were able to see a trend in size change upon binding with heparin.

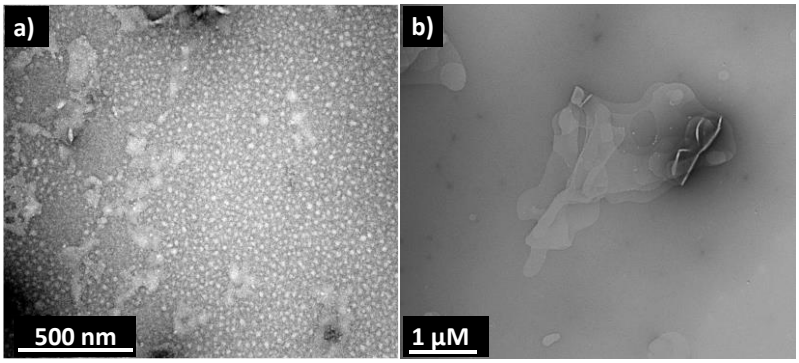

Figure S9. (a) Transmission Electron Microscopy (TEM) images of derivative **1** in the absence a) and presence b) of heparin showing heparin-induced self-assembled 2-dimensional sheet like structure formation of **1**. Concentration of **1** = 0.05 mM; solvent: 50% water in DMSO, concentration of heparin = 25.8 µg/ml and the staining agent = 2% uranyl acetate.

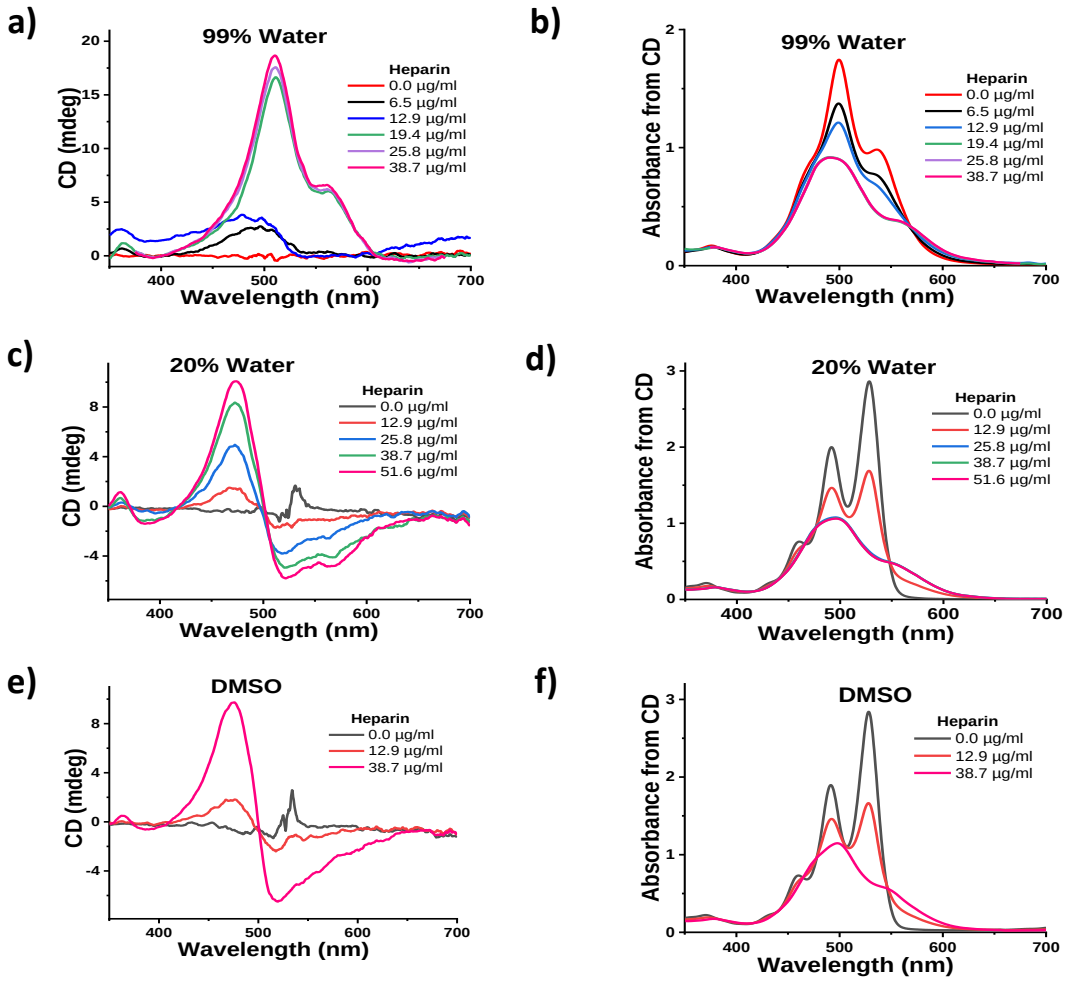

Figure S10. (a) Circular dichroism (CD) and absorption spectra from CD of derivative **1** in 99% water (a, b), 20% water (c,d) and DMSO (f, g) in the absence and presence of various concentrations of heparin. This absorption data collected from CD instrument in the figure differ in absorption intensities from that are recorded on UV-Visible instrument.

As can be seen, the bisignated CD signal only emerge upon decreasing percentage of water in DMSO. In 99% water, we only obtain a monosignated CD signal. This indicates that the enhanced conformatins flexibilty present in samples with lower percentage of water allows helical reorganization upon binding with heparin.

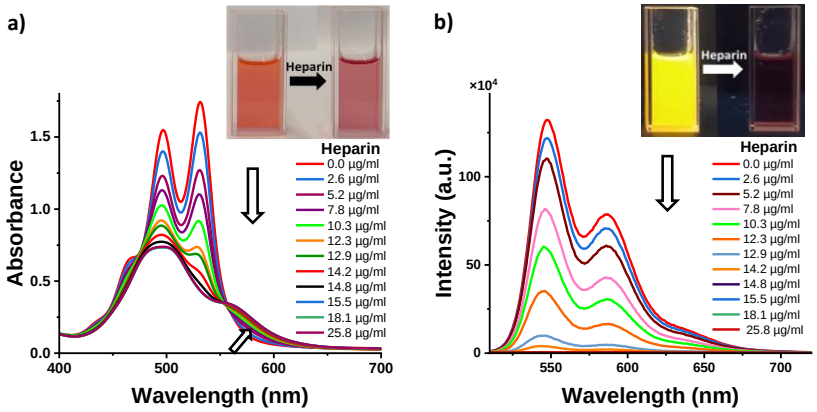

Figure S11. Change in (a) absorption and (b) fluorescence spectra of derivative **1** (0.05 mM) in 50% aqueous medium with gradual increase of heparin concentration at 20 °C (λ_{ex}= 465 nm; slit width (Ex/Em) = 0.5/0.5 nm). [Inset of (a) and (b): Photographs showing colour change of derivative **1** (0.05 mM) before and after the addition of heparin under ambient condition and under 365 nm light].

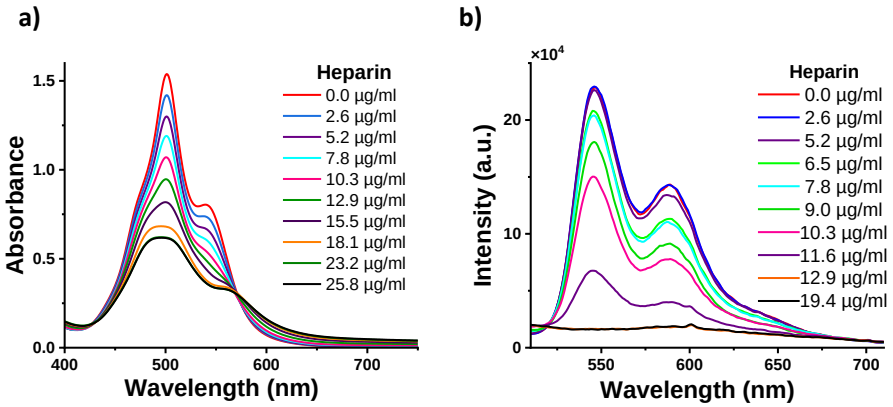

Figure S12. Change in (a) absorption and (b) fluorescence spectra of derivative **1** (0.05 mM) in 99% HEPES buffer (10 mM, pH 7.4) medium with gradual increase of heparin concentration at 20 °C (λ_{ex}= 465 nm; slit width (Ex/Em) = 0.5/0.5 nm).

We performed this experiment in HEPES buffer to rule out any effect of change in pH upon heparin binding.

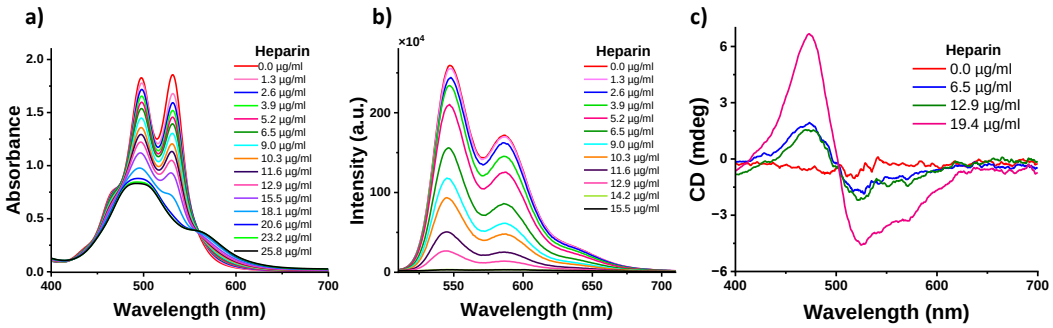

Figure S13. Change in (a) absorption and (b) fluorescence spectra of **1** (0.05 mM) in 50% DMSO-HEPES buffer (10 mM, pH 7.4) with gradual increase of heparin concentration at 20 °C (λ_{ex}= 465 nm; slit width (Ex/Em) = 0.5/0.5 nm).

We performed this experiment in HEPES buffer to rule out any effect of change in pH upon heparin binding.

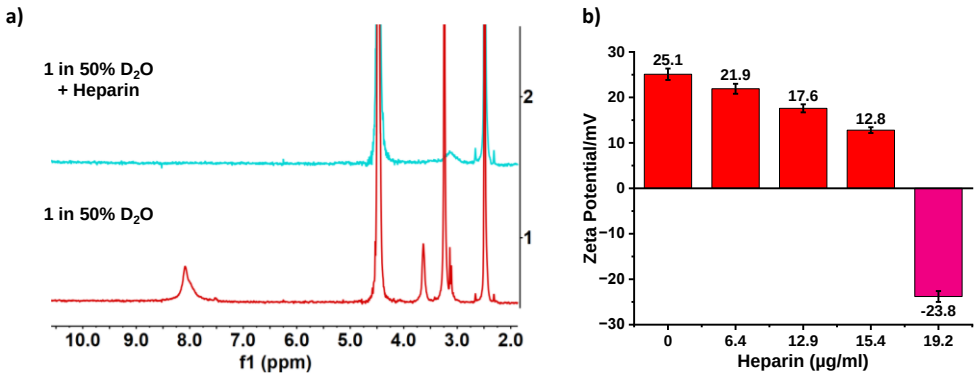

Figure S14. Partial ^{1}H-NMR spectra (stacked) of derivative **1** (1 mM; red line) and **1** (1 mM) + 25.8 mg/ml heparin (blue line) in 50% D_2O-DMSO-d_6 solvent mixture; and (b) variation of zeta potential of derivative **1** (0.05 mM) in the presence of different concentrations of 50% aqueous medium.

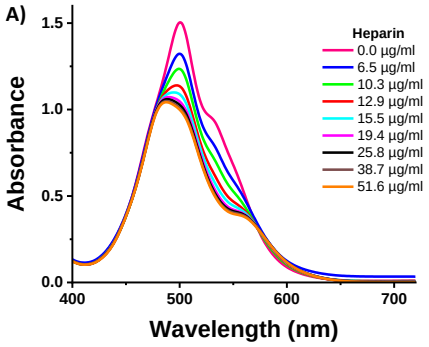

Figure S15. Change in absorption spectra of derivative **1** (0.05 mM) in 50% foetal bovine serum (FBS) with gradual increase of heparin concentration at 20 °C (λ_{ex}= 465 nm; slit width (Ex/Em) = 0.5/0.5 nm).

References

1. R. LeBel and D. Goring, *Journal of Chemical and Engineering Data*, 1962, **7**, 100-101.
2. W. Deng, J. Yu, Y. Qian, R. Wang, Z. Ullah, S. Zhu, M. Chen, W. Li, Y. Guo and Q. Li, *Electrochimica Acta*, 2018, **282**, 24-29.